

EMP Theoretical Notes  
Note 116  
1 March 1971

The Effect of Electron Cascading on  
the Electromagnetic Pulse Generated by a  
High Altitude Burst

Capt. Michael A. Messier  
Air Force Weapons Laboratory

Abstract

Using a simple analytic model, the effect of electron cascading, or avalanching, on the peak fields of the high altitude electromagnetic pulse (EMP) is investigated. From the experimental cascading data presented, it can be seen that the phenomenon should be significant in the 25 km to 40 km altitude region. Analysis shows that the attenuation due to the increased conductivity will reduce the field peak less than an order of magnitude, probably 50 percent or less. However, this increased conductivity could have substantial effect on the late time signal.

## 1. Introduction

This note addresses the question of electron cascading in the upper atmosphere under the influence of the nuclear electromagnetic pulse (EMP). The field strengths predicted by the high altitude burst computer codes indicate that, for certain yields, cascading may be a significant effect. A detailed study is being made with these codes to see under what conditions cascading is important and to what degree. These results will be published separately. This note is an analytic study using step function sources and constant cascading rates. While this approach may not appear useful, since the cascading rate is highly field dependent, it does yield important information related to the relative effects of the various conductivity parameters as well as to the cascading rates that must be produced if cascading is to reduce the peak fields or change the pulse widths.

The high frequency approximation to Maxwell's field equations is used. Cascading is studied in terms of its effect on the time of peak and peak field value. Computer solutions of the same equations are shown so that the influence of cascading on the entire waveform can be observed. Results are plotted in such a way that the separate effects of the cascading rate, electron source rate, and electron mobility can be seen.

## 2. Cascading Data

The cascading rate data used in the computer study, to be published, is shown in figures 1 through 3. This is oxygen data based on measurements made by Phelps.<sup>1</sup> The oxygen data was compared to some nitrogen data<sup>2</sup> and it was found that the Thompson coefficients for each gas were in close agreement for most E/P (electric field/pressure) ratios of interest. The attachment coefficients are higher for oxygen than nitrogen, but the computer studies indicate that attachment plays a very small role in influencing conductivity for the altitudes of interest.

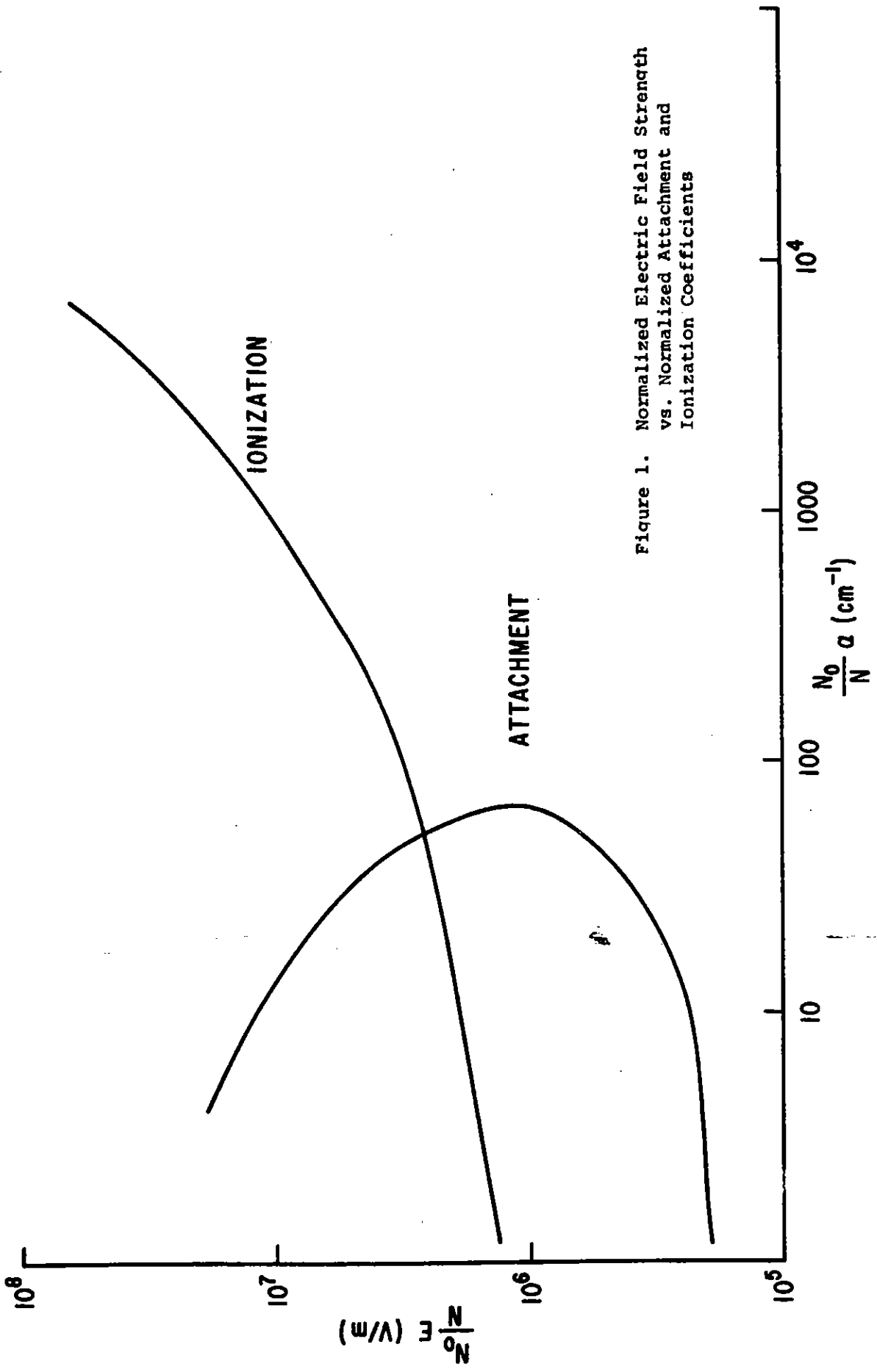


Figure 1. Normalized Electric Field Strength vs. Normalized Attachment and Ionization Coefficients

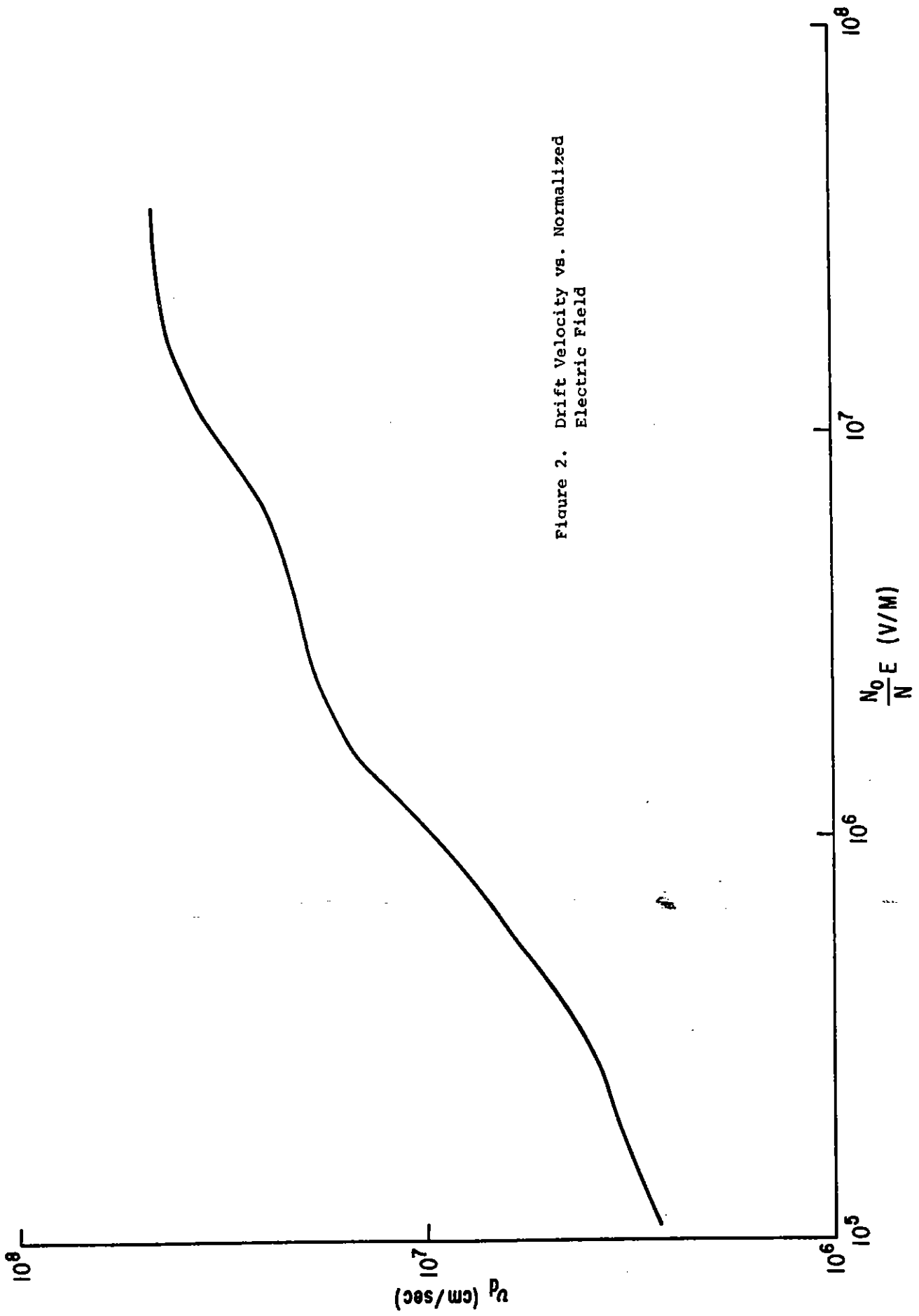


Figure 2. Drift Velocity vs. Normalized Electric Field

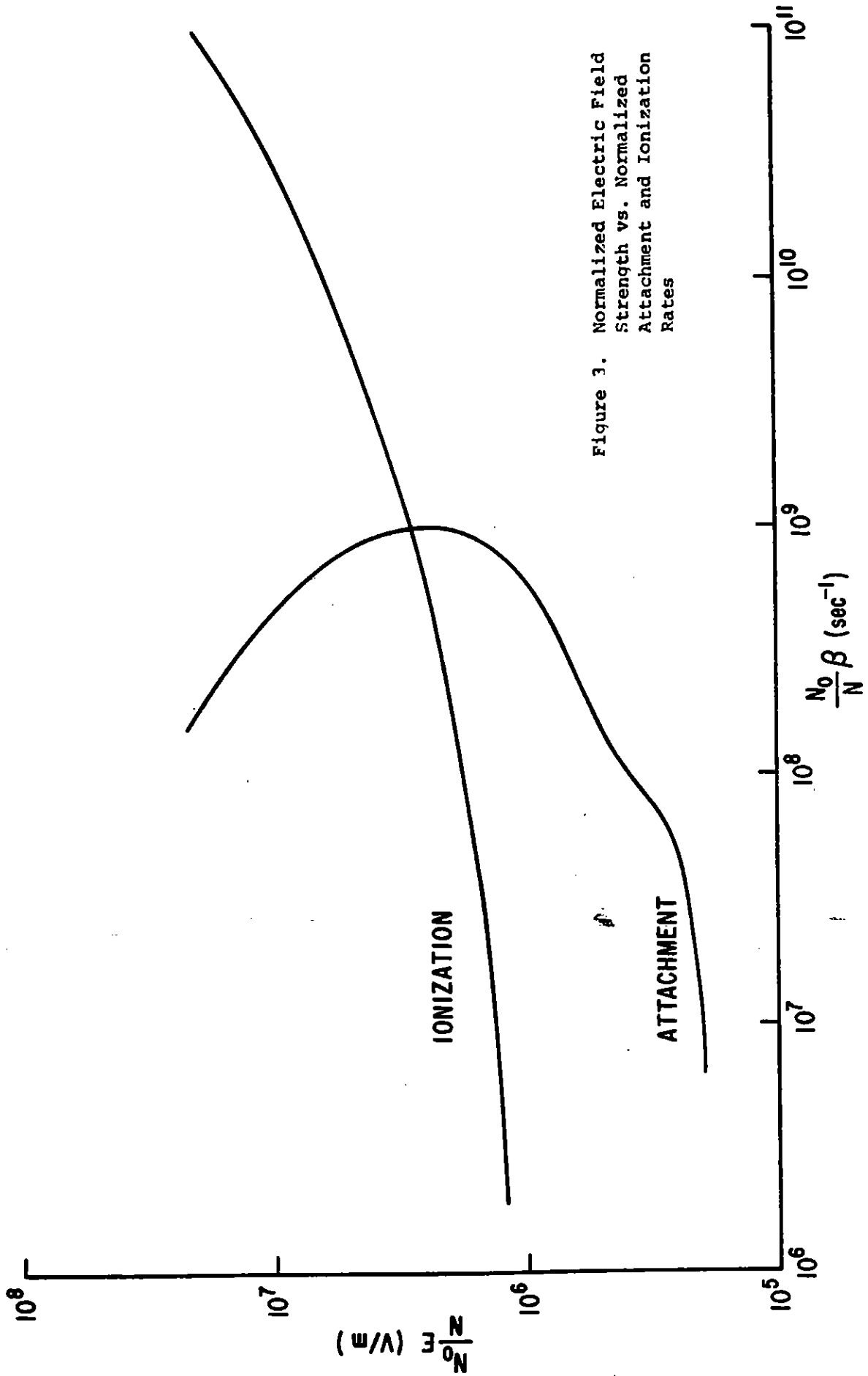


Figure 3. Normalized Electric Field Strength vs. Normalized Attachment and Ionization Rates

Figure 1 shows the Thompson coefficient as a function of electric field strength, both normalized to relative air density. Figure 2 illustrates the drift velocity as a function of the normalized electric field strength. Figure 3 illustrates the ionization and attachment rates as a function of electric field, again with both normalized to relative air density.

### 3. Mathematical Formulation of the Problem

Using the high frequency approximation Maxwell's field equations reduce to (MKS units)

$$\frac{\partial E_r}{\partial \tau} + \frac{\sigma}{\epsilon_0} E_r = \frac{j_r}{\epsilon_0} \quad (3.1)$$

$$\frac{1}{r} \frac{\partial (rE_T)}{\partial r} + \frac{\mu_0 c}{2} \sigma E_T = \frac{\mu_0 c}{2} j_T, \quad (3.2)$$

for the high altitude field, where

$E_r$  = radial electric field

$j_r$  = radial driving current

$E_T$  = transverse electric field

$j_T$  = transverse driving current

$\epsilon_0$  = permittivity of free space ( $8.85 \times 10^{-12}$  farad/m)

$\mu_0$  = permeability of free space ( $4\pi \times 10^{-7}$  henry/sec)

$c$  = speed of light in free space ( $3.00 \times 10^8$  m/sec)

$\sigma$  = conductivity of the media

$\tau$  = local time =  $t - r/c$

$r$  = distance from burst

The conductivity is related to electron density by

$$\sigma = e\mu n \quad (3.3)$$

where

$e$  = electron charge ( $1.602 \times 10^{-19}$  coul)

$\mu$  = electron mobility

$n$  = electron density.

The mobility is electric field dependent. If some type of air chemistry is important, the electron density is both time and field dependent. In reality, the conductivity also depends on the concentrations of the various ionic species, but, for the time frame of interest, these can be neglected because of their relatively low mobility. Since we are considering only cascading (not attachment or recombination), the electron density is given by

$$\frac{dn}{d\tau} = Q + \beta n \quad (3.4)$$

where

$Q$  = electron source rate (elec/sec)

$\beta$  = cascading rate ( $\text{sec}^{-1}$ ).

The cascading rate is field dependent.

For purposes of this discussion, both  $\beta$  and  $\mu$  will be considered field independent. In this case, the conductivity will be strictly time dependent. The set of equations then has the solutions:

$$n(\tau) = \exp\left[\int_0^\tau \beta d\tau\right] \int_0^\tau Q \exp\left[-\int_0^{\tau'} \beta d\tau''\right] d\tau' \quad (3.5)$$

$$\sigma = e\mu n$$

$$E_r(r, \tau) = \exp\left[-\frac{1}{\epsilon_0} \int_0^\tau \sigma d\tau\right] \int_0^\tau \frac{j_r}{\epsilon_0} \exp\left[\frac{1}{\epsilon_0} \int_0^{\tau'} \sigma d\tau''\right] d\tau' \quad (3.6)$$

$$E_T(r, \tau) = \exp \left[ -a \int_0^r \sigma dr \right] \frac{a}{r} \int_0^r r' j_T \exp \left[ a \int_0^{r'} \sigma dr'' \right] dr' , \quad (3.7)$$

where

$$a = \frac{\mu_0 c}{2} = 188 \text{ ohm/m}$$

Alternately, these equations have the form

$$E_r(r, \tau) = \int_0^\tau \frac{j_r}{\epsilon_0} \exp \left[ -\int_{\tau'}^\tau \sigma d\tau'' \right] d\tau' \quad (3.8)$$

$$E_T(r, \tau) = \frac{a}{r} \int_0^r j_T r' \exp \left[ -a \int_{r'}^r \sigma dr'' \right] dr' \quad (3.9)$$

Equation (3.9) sums up all the contributions to the transverse field generated between burst and observer. In high conductivity regions, the skin depth of the plasma is relatively small and the fields seen by the observer are those generated close-by. In this case, the fields can be approximated by integrating from some distance  $r_0$ , instead of  $r = 0$ . Thus,

$$E_T(r, \tau) = \left[ \exp -a \int_{r_0}^r \sigma dr' \right] \frac{r_0}{r} E_0(r_0, \tau) + \frac{a}{r} \int_{r_0}^r j_T r' \exp -a \int_{r'}^r \sigma dr'' dr' . \quad (3.10)$$

In this form, the solution shows the attenuation of the propagated field to be the product of the geometric attenuation and an exponential attenuation due to the conductivity of the region. Near the edge of the deposition region, the current and



conductivity drop to zero and only the geometric attenuation term remains.

Let  $Q$  and  $j_r, j_T$  have step function time dependence and  $1/r^2$  spatial dependence. With  $\beta$  equal to a constant,

$$n = \begin{cases} \frac{Q}{\beta}(e^{\beta\tau}-1) , & \beta > 0 \\ Q\tau , & \beta = 0 \end{cases} \quad (3.11)$$

$$\quad (3.12)$$

for times less than  $\tau_0$ , the pulse duration, and

$$n = \begin{cases} \frac{Q}{\beta} N e^{\beta\tau} , & \beta > 0 \\ Q\tau_0 , & \beta = 0 \end{cases} \quad (3.13)$$

$$\quad (3.14)$$

for times greater than  $\tau_0$ . Here,

$$N = (1 - e^{-\beta\tau_0}) .$$

Because of the  $1/r^2$  dependence, the quantities

$$j_{T0}(\tau) = r^2 j_T(r, \tau) , \quad j_{r0} = r^2 j_r(r, \tau) , \quad (3.15)$$

and

$$\sigma_0(\tau) = r^2 \sigma(r, \tau) \quad (3.16)$$

are constants with respect to  $r$ . The field equations then become

$$E_r(r, \tau) = \exp\left[-\frac{1}{\epsilon_0 r^2} \int_0^\tau \sigma_0 d\tau\right] \frac{1}{\epsilon_0 r^2} \int_0^\tau j_{r0} \exp\left[\frac{1}{\epsilon_0 r^2} \int_0^{\tau'} \sigma_0 d\tau'\right] d\tau' \quad (3.17)$$

$$E_T(r, \tau) = \exp \left[ -a\sigma_0 \int_0^r \frac{dr}{p^2} \right] \left\{ \frac{aj_{T0}}{r} \int_0^r \frac{1}{r'} \exp \left[ a\sigma_0 \int_0^{r'} \frac{dr''}{(r'')^2} \right] dr' \right\} \quad (3.18)$$

during the time the source pulse exists.

Note from the above equations that the radial field is dependent on the time integral of the current, while the transverse field is dependent directly on the current. At the end of the current pulse, the radial field will fall at a rate which varies with the plasma conductivity, but the transverse field will cease immediately. The transverse field at time,  $\tau$ , is the sum of the fields generated between 0 and  $r$ , attenuated by the conductive plasma, at each point's local time,  $\tau$ . The radial field does not propagate.

Assume that the current and conductivity time histories are known at some reference distance,  $R$ . Then  $\sigma_0(\tau) = R^2\sigma(R, \tau)$  and  $j_0(\tau) = R^2j(R, \tau)$ , where the current,  $j$ , is either transverse or radial. During the existence of the driving pulse ( $\tau \leq \tau_0$ ), the radial field is given by

$$E_r(r, \tau) = \begin{cases} \frac{j_{0r}}{\epsilon_0 r^2} e^{-P(\tau)} \int_0^\tau e^{P(\tau')} d\tau', & \beta = 0 \\ \frac{j_{0r}}{\epsilon_0 r^2} e^{-B(\tau)} \int_0^\tau e^{B(\tau')} d\tau', & \beta > 0 \end{cases} \quad (3.19)$$

$$\left( \frac{j_{0r}}{\epsilon_0 r^2} e^{-B(\tau)} \int_0^\tau e^{B(\tau')} d\tau', \quad \beta > 0 \right), \quad (3.20)$$

where

$$j_{r0} = R^2 j_r(R, \tau)$$

$$P(r, \tau) = \frac{R^2 k Q(R)}{2r^2} \tau^2 = \frac{\sigma_0(\beta=0, \tau)}{2\epsilon_0 r^2} \tau$$

$$B(r, \tau) = \frac{R^2 k Q(R)}{r^2 \beta} \left[ \frac{1}{\beta} (e^{\beta \tau} - 1) - \tau \right] = \frac{[\sigma_o(\beta > 0, \tau) - \sigma_o(\beta = 0, \tau)]}{\epsilon_o r^2 \beta}$$

$$k = \frac{e\mu}{\epsilon_o} .$$

After the driving pulse has ceased, the field will decay according to the equations

$$E_r(r, \tau) = \begin{cases} e^{-\alpha_o \tau} E_{ro} , & \beta = 0 \\ \exp(-\alpha e^{\beta \tau}) E_B , & \beta > 0 , \end{cases} \quad (3.21)$$

$$(3.22)$$

where

$$\alpha_o = \frac{\sigma_o(\beta=0, \tau)}{\epsilon_o r^2}$$

$$E_{ro} = \frac{j_{ro}}{\epsilon_o r^2} e^{\gamma_o} \int_0^{\tau_o} e^{P(\tau)} d\tau$$

$$\gamma_o = \frac{\sigma_o(\beta=0, \tau_o)}{2\epsilon_o r^2} \tau_o$$

$$\alpha = \frac{\sigma_o(\beta > 0, \tau)}{\epsilon_o r^2 \beta} e^{-\beta \tau_o}$$

$$E_B = \frac{j_{ro}}{\epsilon_o r^2} e^{\gamma} \int_0^{\tau_o} e^{B(\tau)} d\tau$$

$$\gamma = \frac{\sigma_o(\beta=0, \tau_o)}{\epsilon_o r^2} \tau_o$$

The solution to the transverse field equation has a closed form in terms of the Exponential Integral of the first degree. The Exponential Integral is defined by

$$E_1(x) \equiv \int_x^\infty \frac{e^{-t}}{t} dt . \quad (3.23)$$

The solution of the transverse field is then

$$E_T(r, \tau) = \frac{aj_{T0}}{2} \exp\left(\frac{a\sigma_o}{r}\right) E_1\left(\frac{a\sigma_o}{r}\right) \quad (3.24)$$

Figure 4 shows the function  $E_1(x)$  compared with  $e^{-x}/x$  and  $\ln(1/x)$ . Note that for  $x > 1$ ,

$$E_1(x) \approx \frac{e^{-x}}{x} , \quad (3.25)$$

and for  $x < .8$ ,

$$E_1(x) \approx \ln(1/x) . \quad (3.26)$$

Thus, for  $a\sigma_o/r > 1$ ,

$$E_T(r, \tau) \approx \frac{j_{T0}}{\sigma_o} , \quad (3.27)$$

and, for  $a\sigma_o/r < .8$ ,

$$E_T(r, \tau) \approx \left(\frac{aj_{T0}}{r}\right) e^{\frac{a\sigma_o}{r}} \ln\left(\frac{r}{a\sigma_o}\right) . \quad (3.28)$$

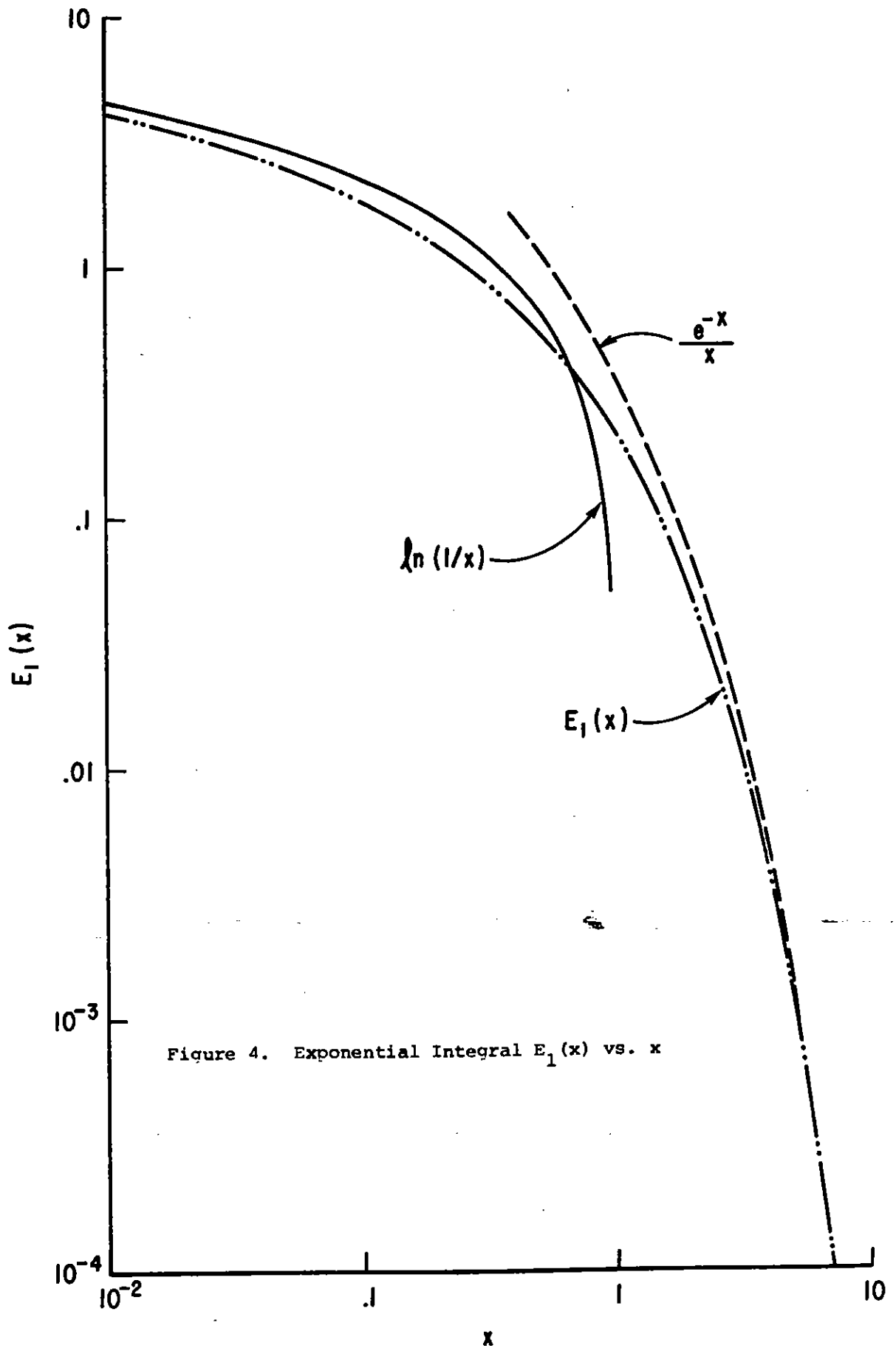


Figure 4. Exponential Integral  $E_1(x)$  vs.  $x$

In the following chapter, we will investigate the variation of the radial field peak with the cascading rate,  $\beta$ . A problem arises with the transverse field generated by a step function current because the field starts at infinity (finite current divided by zero conductivity) and monotonically decreases with increasing conductivity. There is no field peak without a time dependent current. It is instructive to calculate the value of current time derivative,  $j'_{T0}$ , at the time the field peaks. If the conductivity remains small or does not vary, the field would follow the current time history and peak when  $j'_{T0} = 0$ . Normally, however, it will peak when

$$j'_{T0} = \frac{aj_{T0}\dot{\sigma}_0}{r} \left[ \frac{r}{a\sigma_0 \exp\left(\frac{a\sigma_0}{r}\right) E_1\left(\frac{a\sigma_0}{r}\right)} - 1 \right]. \quad (3.29)$$

For large conductivities ( $a\sigma_0/r \gg 1$ ), this formula again reduces to  $j'_{T0} = 0$  as the field equation reduces to  $j_{T0}/\sigma_0$ .

#### 4. Variation of Radial Peak in Time

The peak radial field occurs when the conduction current equals the driving current, ie,

$$\sigma E_r = j_r, \quad (4.1)$$

or

$$E_r = \frac{j_r}{e\mu n}. \quad (4.2)$$

Time will be divided into two regimes:  $\tau < 1/\beta$ , when cascading does not dominate, and  $\tau \geq 1/\beta$ , when cascading dominates.

In the first case, and when  $\beta = 0$ ,

$$n = Q\tau \quad (4.3)$$

and

$$\int_0^{t_p} e^P d\tau = \frac{e^{P(t_p)}}{kn_0(t_p)}, \quad (4.4)$$

where

$$P = \frac{k}{2} Q\tau^2 = \frac{kn_0(\tau)\tau}{2}$$

$$k = \frac{e\mu}{\epsilon_0}$$

$t_p$  = time of field peak

$n_0$  = electron density without cascading ( $Q\tau$ )

Changing the variable of integration from  $\tau$  to  $P$ ,

$$\int_0^{P(t_p)} \frac{e^P}{P} dP = \frac{e^{P(t_p)}}{kn_0(t_p)}, \quad (4.5)$$

where  $P = kQ\tau = kn_0(\tau)$ .

Utilizing the Mean Value Theorem of integral calculus to pull the linear term through the integral,

$$\int_0^{P(t_p)} e^P dP = \frac{\bar{t}}{t_p} e^{P(t_p)}. \quad (4.6)$$

Choose the intermediate value,  $\bar{t}$ , to be  $t_p/2$ , then

$$t_p \approx \sqrt{\frac{2kn_0^2}{kQ}} \approx \frac{1}{\sqrt{kQ}}. \quad (4.7)$$

This equation can be used to find the range of  $Q$  which allows  $t_p < \beta^{-1}$ , namely,

$$Q > \beta^2/k . \quad (4.8)$$

Table 4.1 gives the minimum Q necessary as a function of  $\beta$  and  $\mu$ .

$\beta \backslash \mu$	$10^7$	$3 \cdot 10^7$	$5 \cdot 10^7$	$10^8$
1	$5.5(10^{21})$	$4.9(10^{22})$	$1.4(10^{23})$	$5.5(10^{23})$
2	$2.8(10^{21})$	$2.5(10^{22})$	$7.0(10^{22})$	$2.8(10^{23})$
5	$1.1(10^{21})$	$9.9(10^{21})$	$2.8(10^{22})$	$1.1(10^{23})$
10	$5.5(10^{20})$	$4.9(10^{21})$	$1.4(10^{22})$	$5.5(10^{22})$
20	$2.8(10^{20})$	$2.5(10^{21})$	$7.0(10^{21})$	$2.8(10^{22})$

Table 4.1

Values of Q Necessary for  $t_p < \beta_i^{-1}$

When cascading dominates, equation 4.4 becomes

$$\int_0^{t_p} e^{B(\tau)} d\tau = \frac{e^{B(t_p)}}{kn(t_p)} \quad (4.9)$$

where

$n$  = electron density with cascading

$$= \frac{Q}{\beta}(e^{\beta\tau} - 1)$$

$$B = \frac{k}{\beta}(n - n_0),$$

where  $n_0$  is the value of  $n$  which would be seen if cascading did not occur. Following the above procedure,



$$\int_0^{B(t_p)} \frac{e^B}{\dot{B}} dB = \frac{e^{B(t_p)}}{kn(t_p)}, \quad (4.10)$$

where

$$\dot{B} = \frac{kQ}{\beta} (e^{\beta\tau} - 1) = kn(\tau),$$

and

$$\int_0^{B(t_p)} e^B dB = \frac{\bar{n}}{n} e^{B(t_p)}, \quad (4.11)$$

where  $\bar{n}$  is an intermediate value of  $n$ .

The quantity  $\bar{n}$  can be approximated by calculating  $n$  as a function of some representative value of time  $\bar{t}$ . When calculating the  $\beta = 0$  case, we used  $\bar{t} = t_p/2$  because  $n$  was a linear function of time. In this case,  $n$  is nearly an exponential function of time, so that  $\bar{t}$  can be expected to be weighted to times larger than  $t_p/2$ . For large  $\beta t_p$ ,  $n$  can be approximated by

$$n = n' e^{\beta\tau}, \quad (4.12)$$

with  $n'$  constant. Then, define

$$\bar{n} = n' \frac{\int_{t'}^{t_p} e^{\beta\tau} d\tau}{t_p - t'}, \quad (4.13)$$

where  $t'$  is some time when  $n'$  was equal to the electron density (before cascading became important). For  $t_p \gg t'$ ,

$$\bar{n} = n' \frac{e^{\beta t_p}}{\beta t_p} . \quad (4.14)$$

Substituting 4.14 into 4.12,

$$\bar{t} = t_p - \frac{1}{\beta} \ln \beta t_p , \quad (4.15)$$

or

$$\frac{\bar{t}}{t_p} = 1 - \frac{\ln(\beta t_p)}{\beta t_p} . \quad (4.16)$$

Typical values are  $\beta = 10^8$  and  $t_p = 3 \cdot 10^{-8}$ , so that

$$\bar{t} = \frac{2}{3} t_p . \quad (4.17)$$

Now,

$$\frac{\bar{n}}{n} = \frac{e^{\beta \bar{t}} - 1}{e^{\beta t_p} - 1} ,$$

or, for large  $\beta t_p$ ,

$$\frac{\bar{n}}{n} = \exp(-\beta(t_p - \bar{t})) = \exp\left(-\frac{\beta}{3} t_p\right) . \quad (4.18)$$

Then,

$$e^{B(t_p)} = \frac{1}{1 - \exp\left(-\frac{\beta}{3} t_p\right)} \approx 1 + \exp\left(-\frac{\beta}{3} t_p\right) . \quad (4.19)$$

Continuing,

$$B(t_p) = \ln\left(1 + \exp\left(-\frac{\beta}{3} t_p\right)\right) \approx \exp\left(-\frac{\beta}{3} t_p\right) . \quad (4.20)$$

For  $n \gg n_0$ , ie, significant cascading,

$$\frac{kQ}{\beta^2} (e^{\beta t_p} - 1) = e^{-\frac{\beta}{3} t_p} \quad (4.21)$$

or

$$t_p = \frac{3}{4\beta} \ln\left(\frac{\beta^2}{kQ} + 1\right) \quad (4.22)$$

Using the equality,

$$Q_0 = \epsilon \mu R^2 Q(R) , \quad (4.23)$$

equation 4.22 becomes

$$t_p = \frac{3}{4\beta} \ln\left(\frac{\epsilon_0 \beta^2 r^2}{Q_0} + 1\right) \quad (4.24)$$

The field value at the peak can be found by substituting the value of the peak time back into

$$E_r = \frac{j_{r0}}{\sigma_0} \tau_p . \quad (4.25)$$

With cascading, then,

$$E_r(\tau_p) = \frac{j_{ro}\beta}{Q_o} \left[ \left( \frac{\epsilon_o\beta^2 r^2}{Q_o} + 1 \right)^{3/4} - 1 \right] \quad (4.26)$$

$$E_r(\tau_p) \approx \frac{j_{ro}}{\left[ Q_o\beta^2 (\epsilon_o r^2)^3 \right]^{1/4}}, \quad (4.27)$$

for

$$\frac{\epsilon_o\beta^2 r^2}{Q_o} \gg 1 .$$

The peak field varies inversely as the square root of  $\beta$  and is inversely proportional to  $r^{3/2}$ .

Table 4.2 compares the peak times calculated by computer, using the radial field integral equation, and the approximate peak times calculated using equation 4.22. Note that this equation starts breaking down near  $\beta = 3.10^7$ .

$\beta$ (sec <sup>-1</sup> )	$t_p$ (sh)	Approximate $t_p$ (sh)
$10^8$	3.1	3.0
$5.10^7$	4.1	4.0
$3.10^7$	5.0	4.5
$10^7$	6.3	3.3

Table 4.2

Actual and Approximate Peak Times

## 5. Time Waveforms

This section presents computer calculations of the effects of cascading using the same equations developed for the previous analytic study. The radial equations (equations 3.19 and 3.20) were integrated as simple summations of the form

$$E_r(r, \tau) = \frac{j_{or}}{\epsilon_0 r^2} e^{-P(\tau)} \sum_i \left[ e^{P(\tau_i)} \Delta\tau \right]. \quad (5.1)$$

The transverse fields were calculated using equation 3.24 and a polynomial expansion of the exponential integral for  $a\sigma_0/r < 1$ , and using equation 3.27 otherwise.

Three separate parameter studies were made with both the radial and transverse equations. In each case, a current of 10 amp/m<sup>2</sup> was used. The first study is a variation of the cascading rate using a mobility of 10 m<sup>2</sup>/V-sec and an electron production rate of 10<sup>21</sup> elec/m<sup>3</sup>-sec. The cascading rate is varied from 0 to 10<sup>8</sup> sec<sup>-1</sup>. The second study is a variation of the electron production rate using cascading rates of 0 and 3 × 10<sup>7</sup> sec<sup>-1</sup> and a mobility of 10 m<sup>2</sup>/V-sec. Finally, a study of the mobility dependence is made using cascading rates of 0 and 3 × 10<sup>7</sup> sec<sup>-1</sup> and an electron production rate of 10<sup>21</sup> elec/m<sup>3</sup>-sec.

Figure 5 shows the conductivity history for various rates of cascading. Because of the semi-log scale, one can see when cascading dominates by noting when the curves become straight lines. Figure 6 shows the variation of the time waveform with cascading rate, and figure 7 illustrates the ratio of each of the fields affected by cascading to the field not so affected. Figures 8 and 9 depict the production rate and mobility studies, respectively. Figures 10 through 13 show the same comparisons, in order, for the transverse field.

Figure 5. Conductivity vs. Time For Various Cascading Rates

$$Q = 10^{21} \text{ elec/m}^3\text{-sec}$$

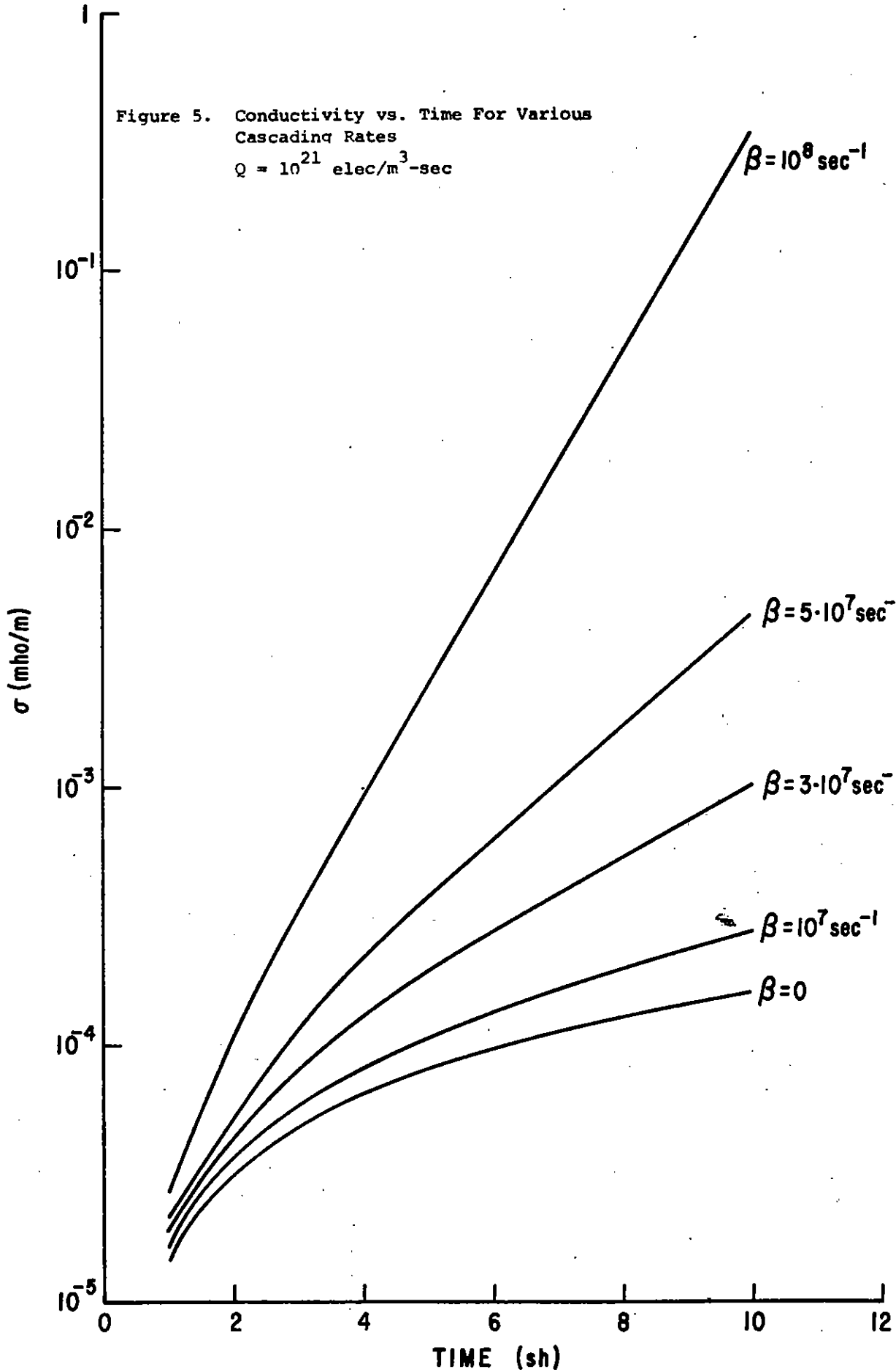
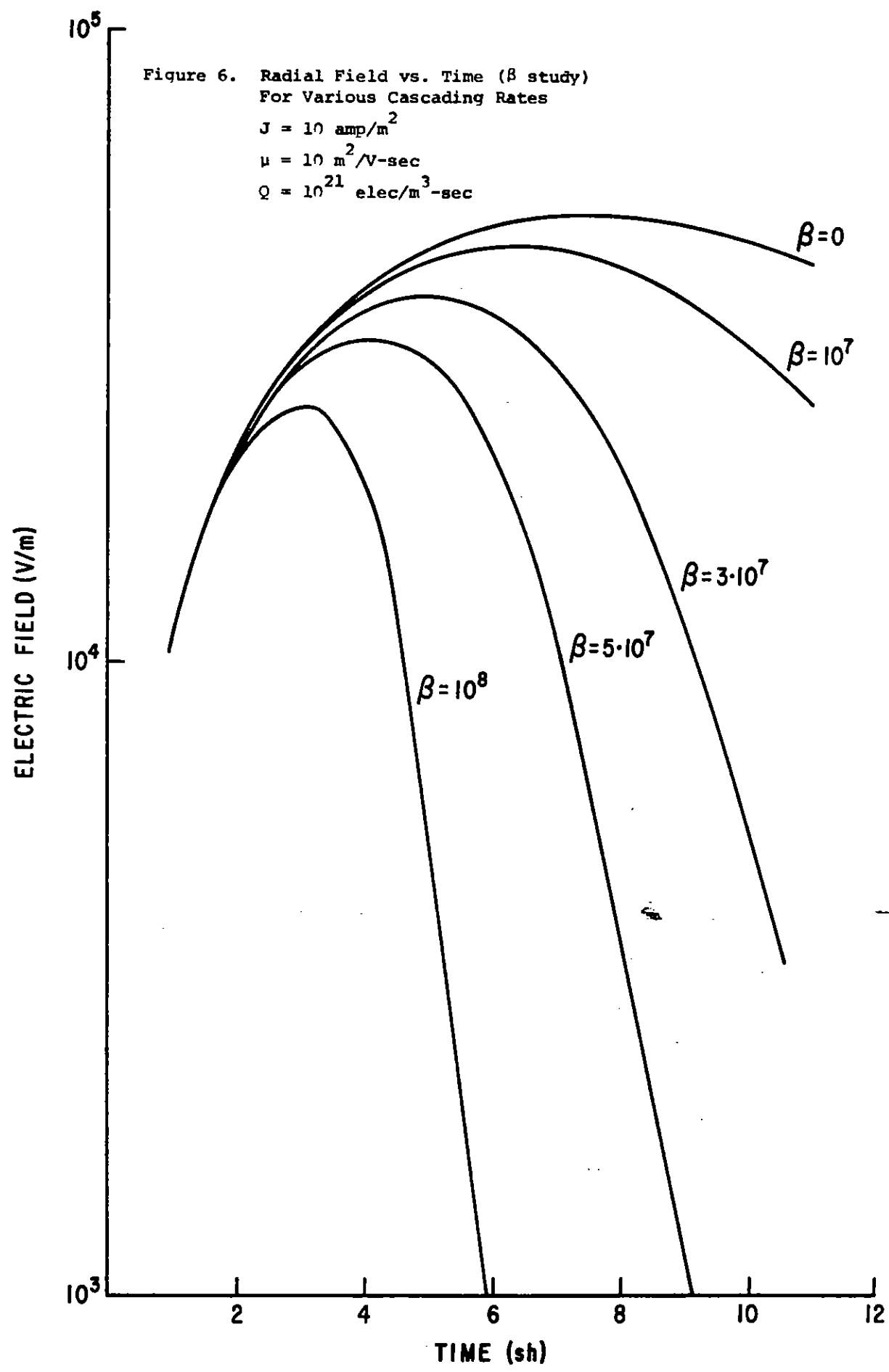
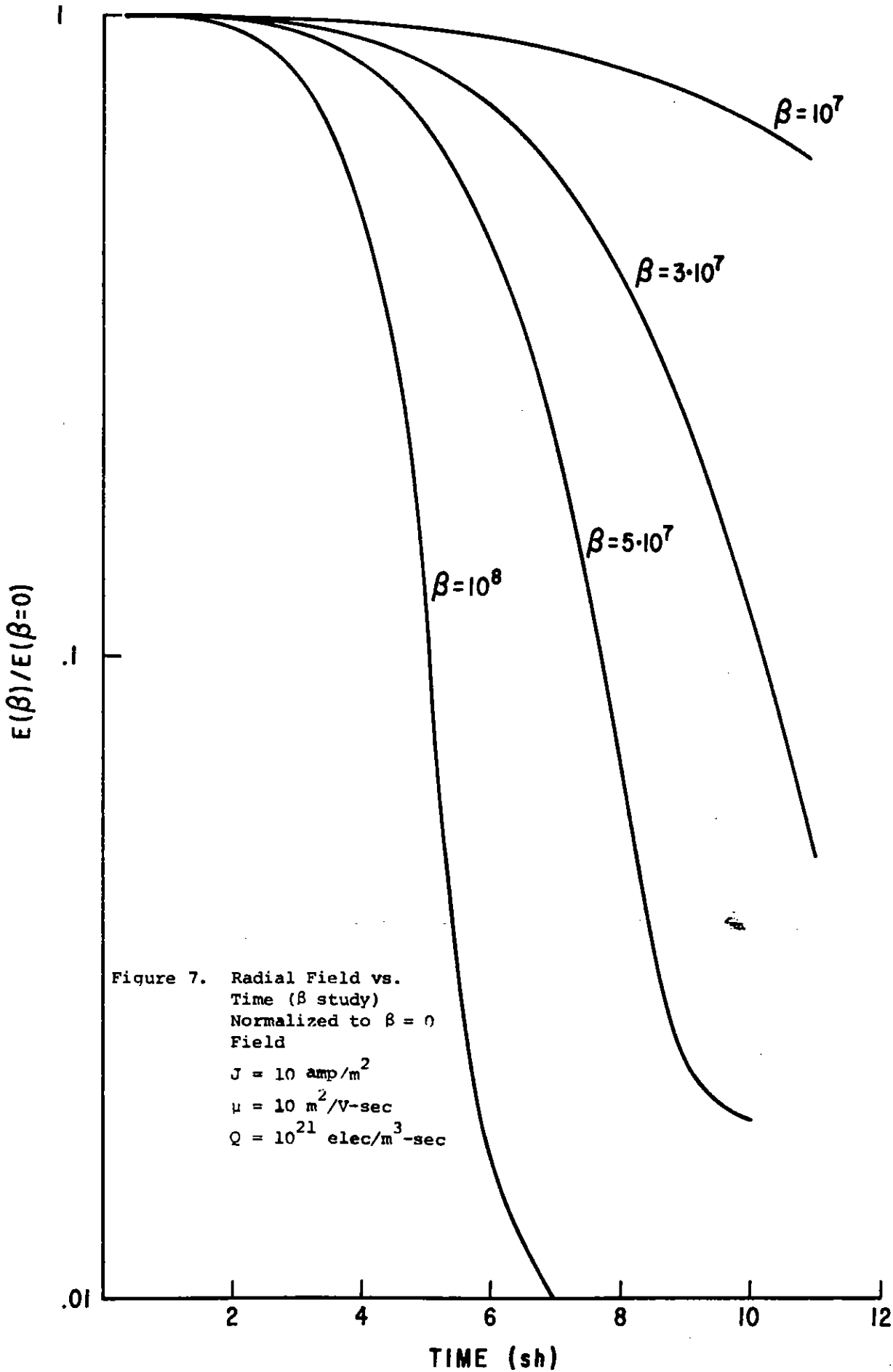


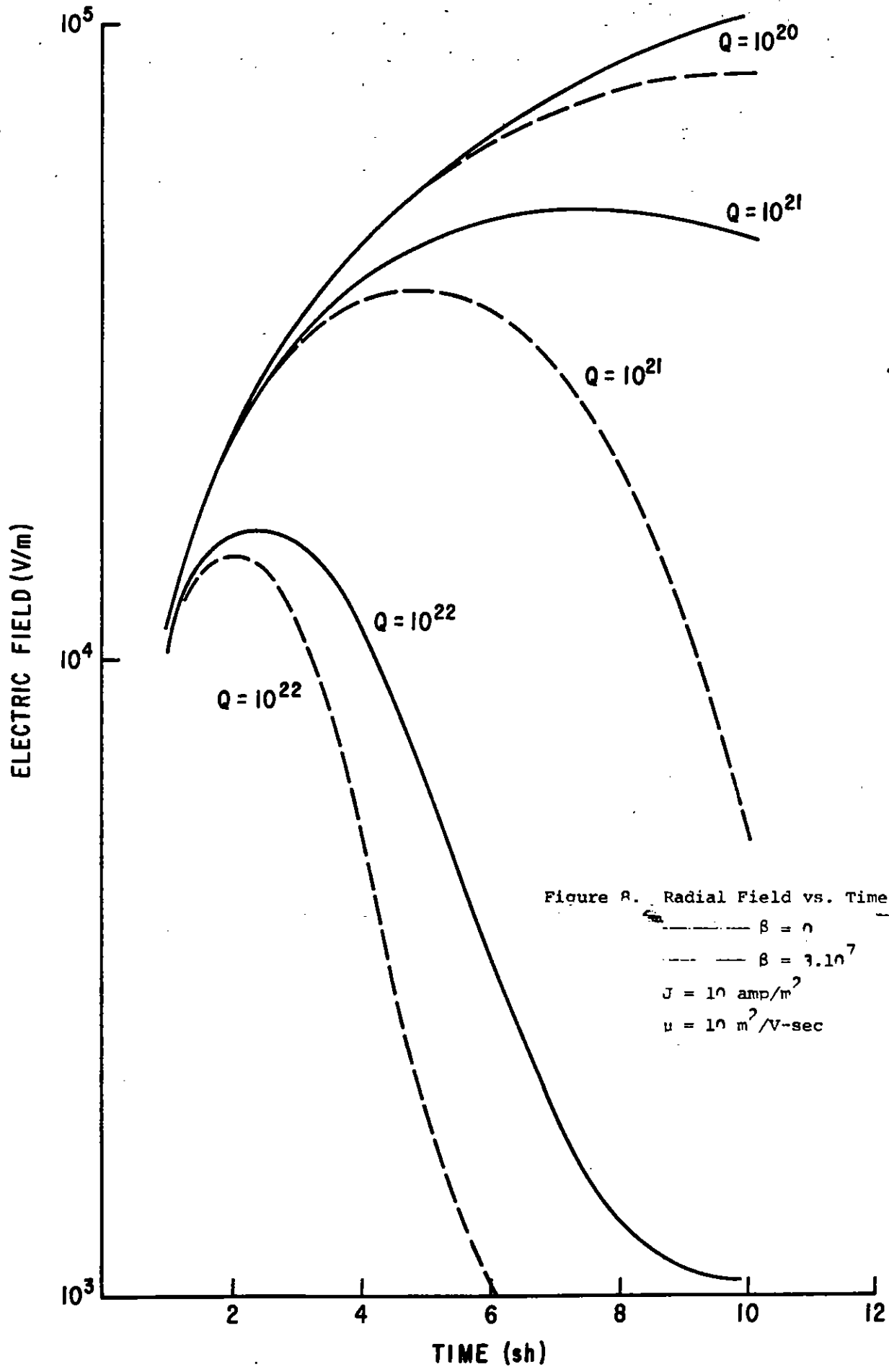
Figure 6. Radial Field vs. Time ( $\beta$  study)  
For Various Cascading Rates

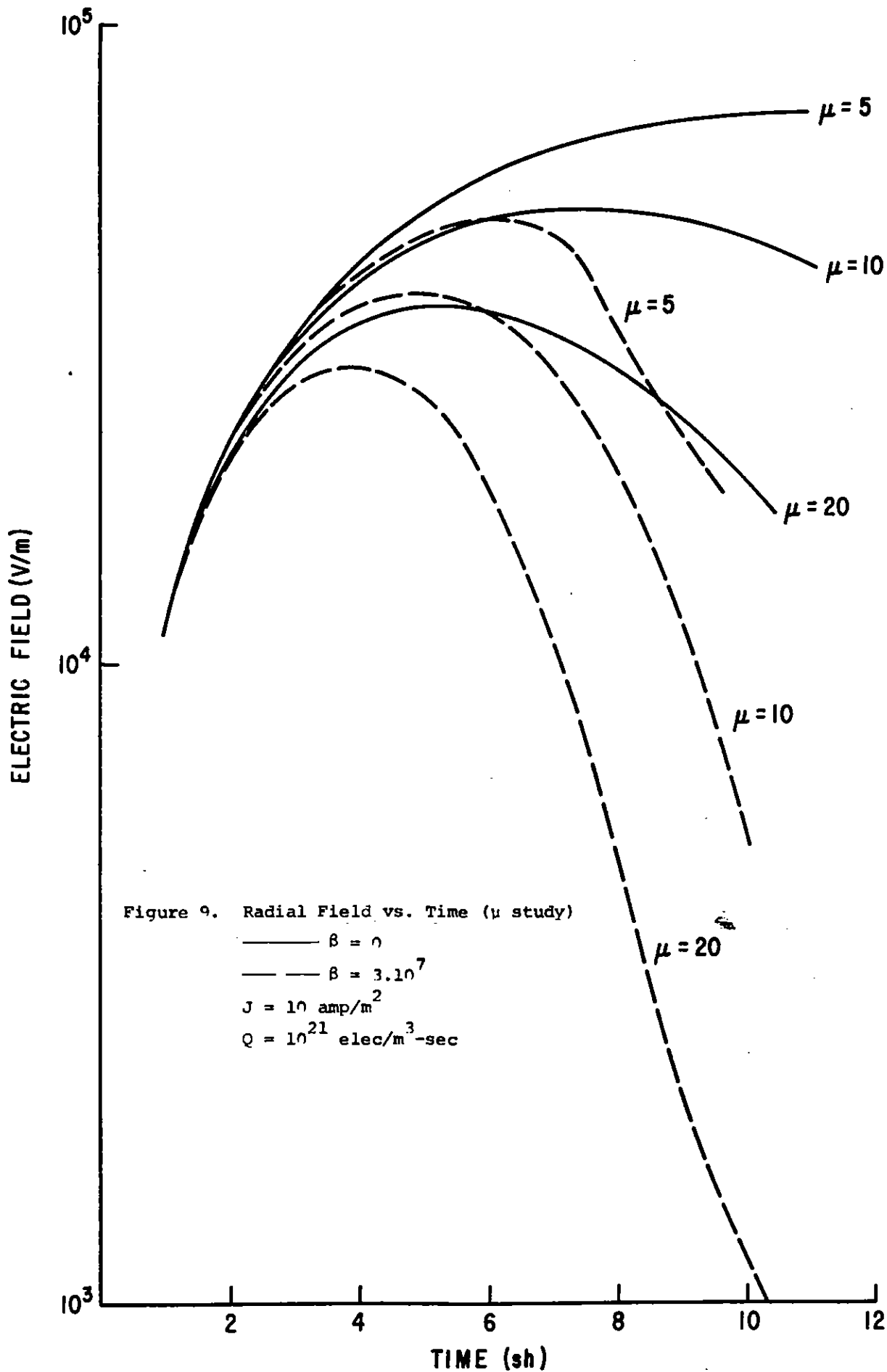
$J = 10 \text{ amp/m}^2$   
 $\mu = 10 \text{ m}^2/\text{V-sec}$   
 $Q = 10^{21} \text{ elec/m}^3\text{-sec}$

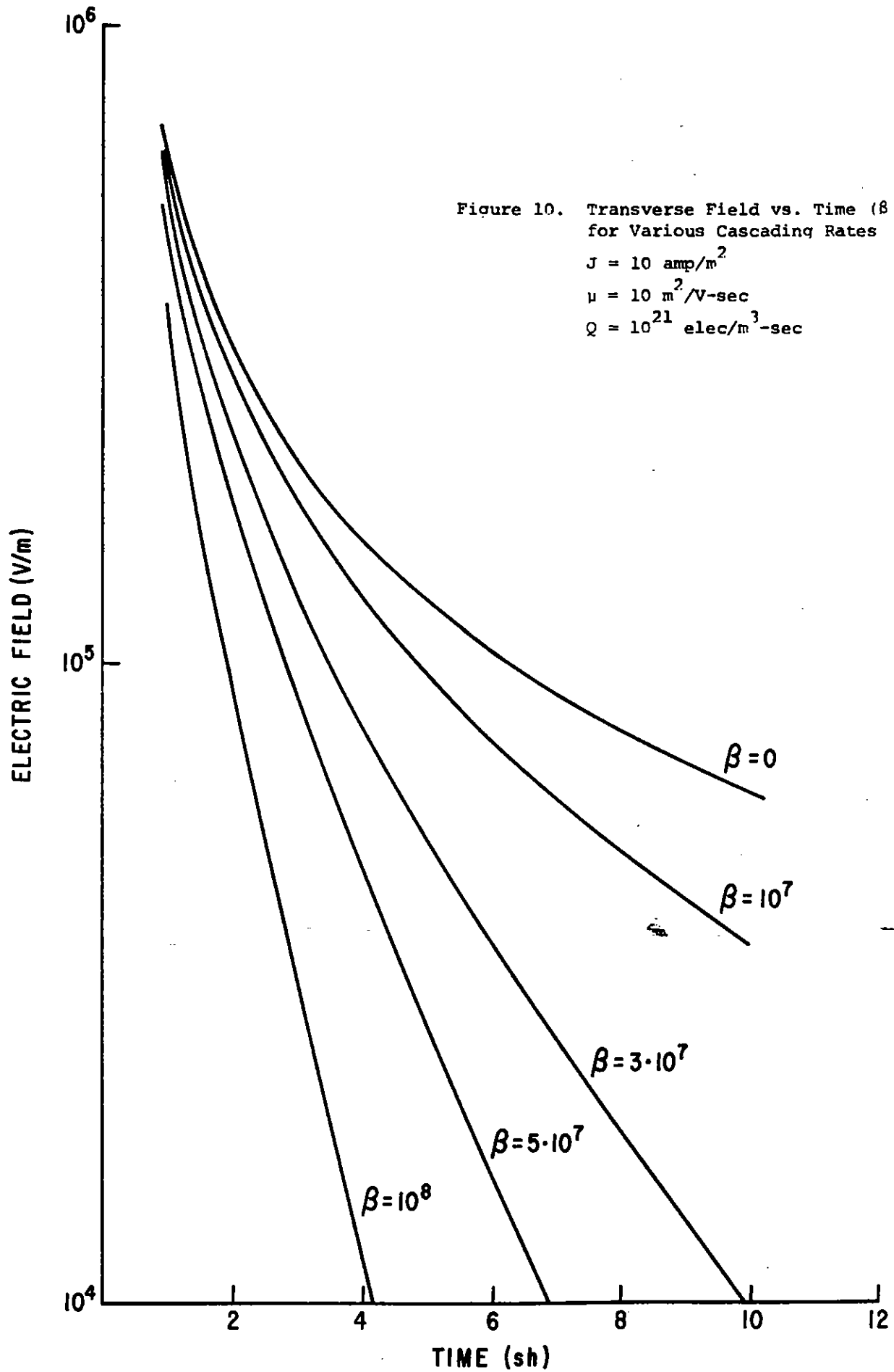












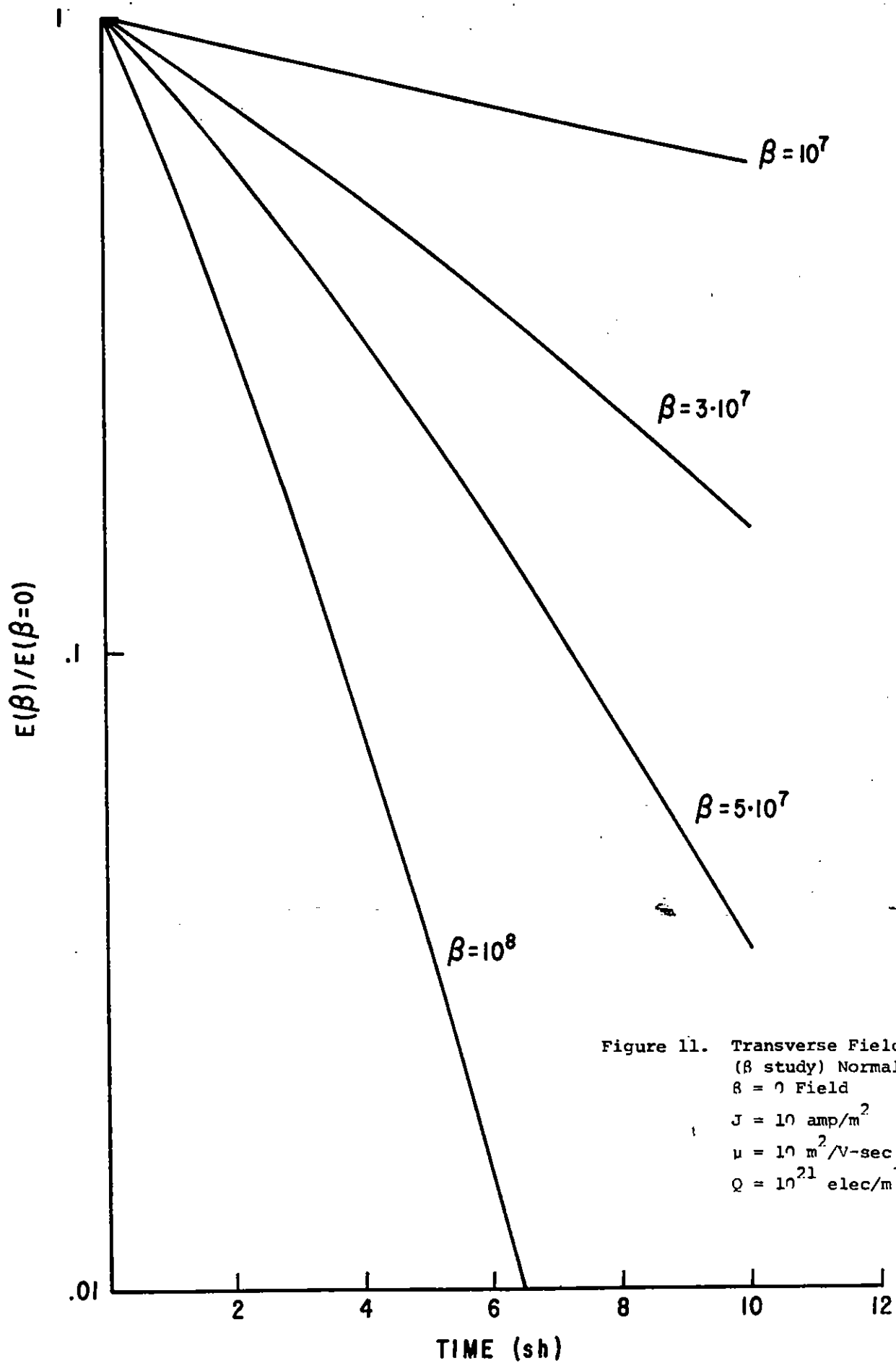


Figure 11. Transverse Field vs. Time  
 ( $\beta$  study) Normalized to  
 $\beta = 0$  Field  
 $J = 10 \text{ amp/m}^2$   
 $\mu = 10 \text{ m}^2/\text{V-sec}$   
 $Q = 10^{21} \text{ elec/m}^3\text{-sec}$

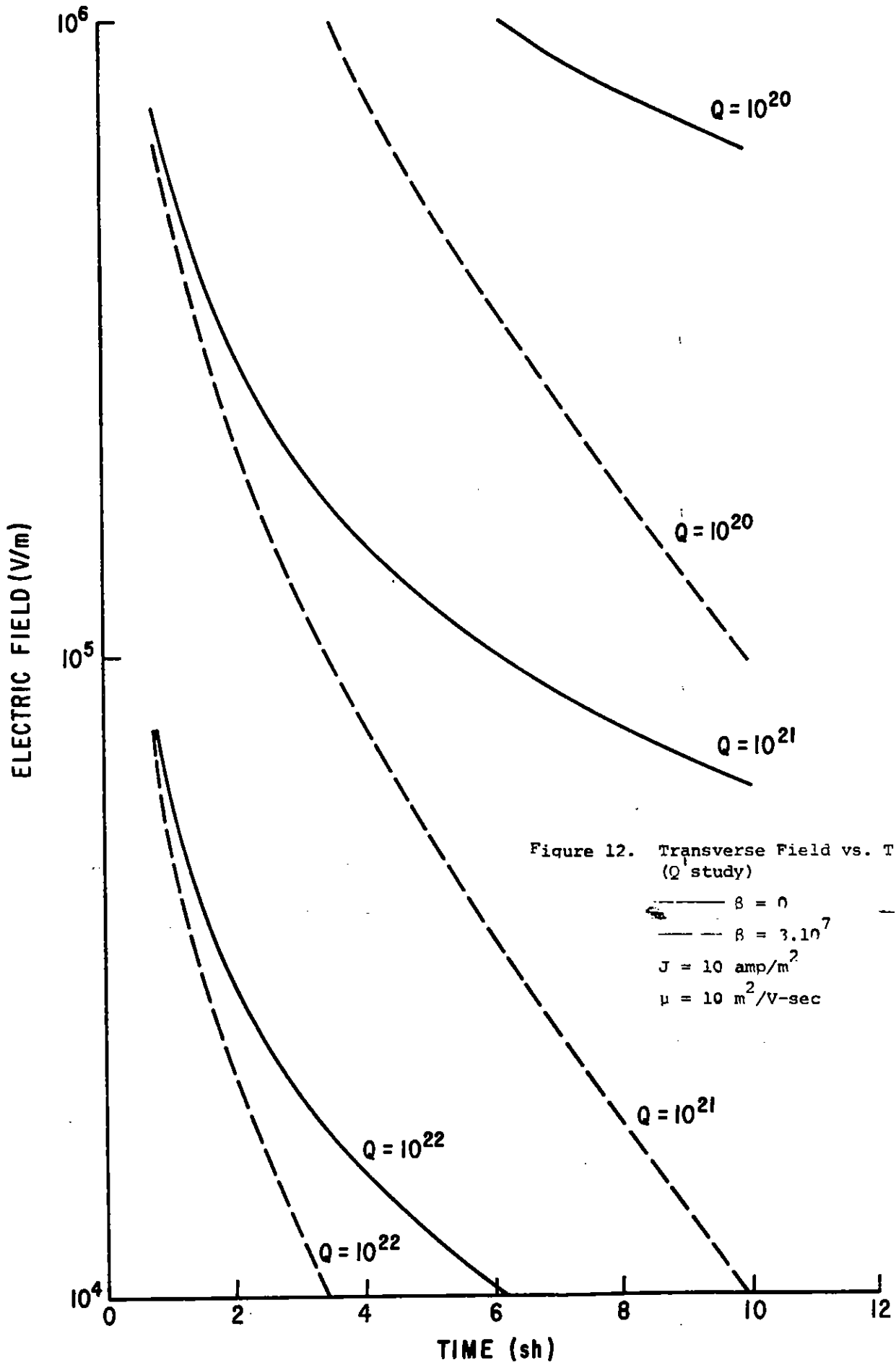
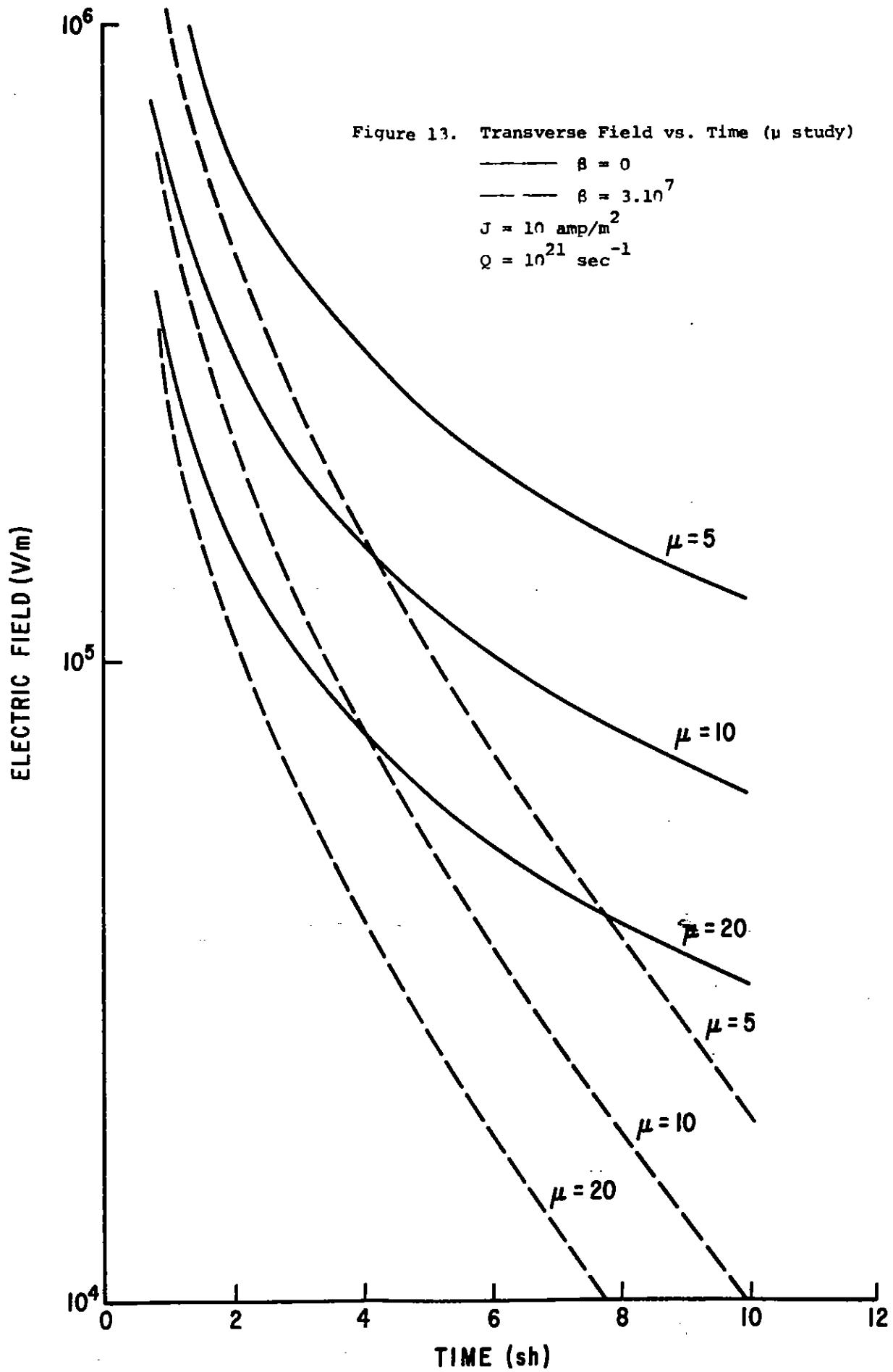


Figure 13. Transverse Field vs. Time ( $\mu$  study)



## 6. Discussion and Conclusion

While the preceding analysis does not reflect a real situation, its simplicity serves to isolate the various factors involved, eg, the relative importance of electron source rate, cascading rate, and mobility. The cascading rate and drift velocity can be identified with altitude and electric field strength through the data in chapter 2. From this analysis it is possible to draw some general conclusions about the effects of cascading on a real pulse.

If cascading is to be effective, it must have significantly altered the electron density before or shortly after the field peak. After the peak, the cascading rate will drop and becomes less influential. If  $t_p$  is the time to the field peak and if an e-fold increase in electron density is considered significant, then an average value of  $\beta$  equal to  $1/t_p$  will give the desired results. In the deposition region, field peaks normally occur in the 3 to 6 shake region, implying that average cascading rates on the order of  $2$  or  $3 \times 10^7 \text{ sec}^{-1}$  are necessary. For purposes of this discussion, we will approximate the average value of  $\beta$  by the value of  $\beta$  corresponding to the average field strength, ie,

$$\overline{\beta(E)} \equiv \beta(\overline{E}) . \quad (6.1)$$

As a first approximation in calculating  $\overline{E}$ , consider the average field (to peak) of a double exponential time waveform,

$$E = E_0 (e^{-\gamma t} - e^{-\alpha t}) . \quad (6.2)$$

The approximation is good when cascading produces a small change in electron density. The time to peak of such a waveform is

$$t_p = \frac{\ln(\alpha/\gamma)}{(\alpha-\gamma)} . \quad (6.3)$$

In most cases of interest,  $\alpha \gg \gamma$ , so that 6.3 becomes

$$t_p = \frac{1}{\alpha} \ln(\alpha/\gamma) . \quad (6.3a)$$

The peak field is given for  $\alpha \gg \gamma$  by

$$E_p = E_o \left(\frac{\gamma}{\alpha}\right)^{\gamma/\alpha} \left(1 - \frac{\gamma}{\alpha}\right) \quad (6.4)$$

Figure 14 shows  $E_p/E_o$  as a function of  $\alpha/\gamma$ . The average field to peak is then given by

$$\bar{E} = \frac{E_o}{t_p} \int_0^{t_p} (e^{-\gamma t} - e^{-\alpha t}) dt , \quad (6.5)$$

or

$$\bar{E} = E_p \frac{\left(\frac{\alpha}{\gamma}\right)^{\gamma/\alpha}}{\left(1 - \frac{\gamma}{\alpha}\right) \left[1 - \frac{1}{\ln\left(\frac{\gamma}{\alpha}\right)}\right]} . \quad (6.6)$$

Figure 14 also shows a plot of  $\bar{E}/E_p$  as a function of  $\alpha/\gamma$ . Note that

$$\bar{E} = .8 E_p$$

is a good approximation.

The peak fields at thirty or forty kilometers altitude, from a weapon larger than about 100 kT and above 50 km, are sufficient to produce cascading with the air density present. In fact, by considering typical field values and the data in chapter 2, one can expect a cascading frequency,  $\beta$ , of  $10^8 \text{ sec}^{-1}$ .



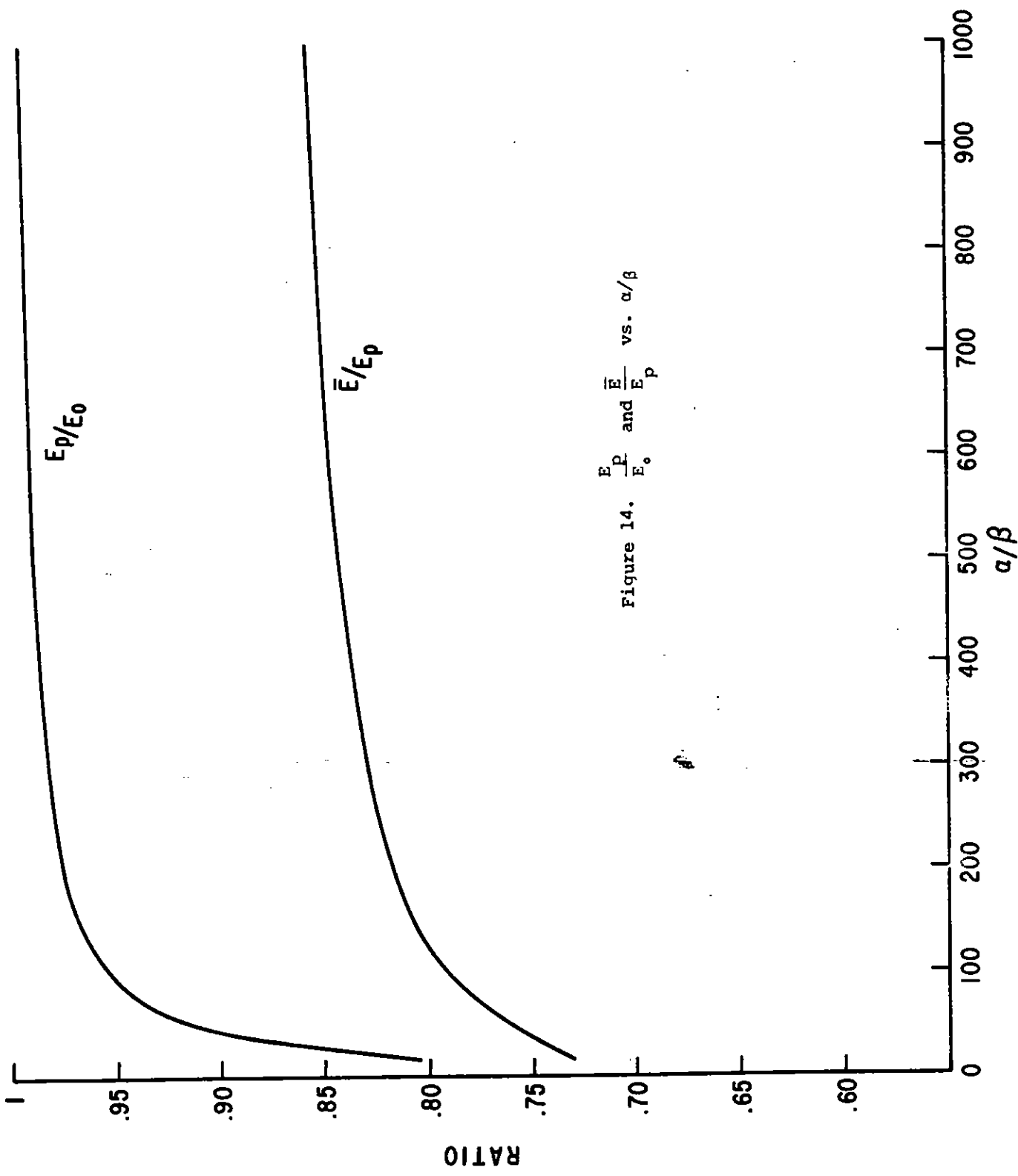


Figure 14.  $\frac{E_p}{E_0}$  and  $\frac{\bar{E}}{E_p}$  vs.  $a/\beta$

The transverse fields will be more influenced than the radial fields because they must propagate through a region of increased conductivity as well as be generated within it. In the deposition region, the ratio of transverse field to radial field depends on the angle between the line of sight and the earth's magnetic field. Thus, the relative impact of cascading will vary throughout the deposition region, as well as over the surface of the earth. Based on the preceding analysis and also on some analysis with the high altitude code HEMP (to be published), it appears that peak fields can be affected by 50%. This is not extremely important in itself, but the increased falloff of the fields could significantly alter the low and medium frequency content of the signal.

#### References

1. Phelps, A. V., and W. H. Kasner, AFWL-TR-66-34, "Studies and Experimental Work on Atomic Collision Processes Occurring in Atmospheric Gases," Air Force Weapons Laboratory, 1966 (Unclass.).